Revue des Composites et des Matériaux Avancés-Journal of Composite and Advanced Materials
Vol. 35, No. 2, April, 2025, pp. 381-389
Journal homepage: http://iieta.org/journals/rcma

Comparative Analysis of ANFIS-PSO and ANFIS-GA Predictions for MRR in AL-8112 Alloy Machining

Imhade P. Okokpujie[1,2*], Muhammad I. N. Ma'arof[2], Aderonke O. Akinwumi[1], Remilekun R. Elewa[1], Stella I. Monye[1], Kennedy Okokpujie[3]

[1] Department of Mechanical and Mechatronics Engineering, Afe Babalola University, Ado Ekiti 360001, Nigeria
[2] Mechanical Engineering Department, INTI International University, Nilai 71800, Malaysia
[3] Department of Electrical and Information Engineering, College of Engineering, Covenant University, Ota 112104 Nigeria

Corresponding Author Email: ip.okokpujie@abuad.edu.ng

https://doi.org/10.18280/rcma.350220

Received: 7 January 2025
Revised: 12 February 2025
Accepted: 20 February 2025
Available online: 30 April 2025

Keywords:
ANFIS-PSO, ANFIS-GA, AL-8112 alloy, material removal rate, machining, precision, hybrid modeling

ABSTRACT

The ability to predict MRR due to its significance in machining operations cannot be underestimated. Most computer numerical control cutting tools do not withstand high MRR during operation because they cause high heat generation and friction. This leads to high vibrations by chip discontinuity with material adhesion. The high vibration increases the cutting tool wear rate and leads to the cutting tool's substitution. Therefore, this study focuses on the comparative study of the prediction performance of ANFIS-PSO and ANFIS-GA of MRR via machining of Al-8112 alloy. The machining operation was carried out under the TiO_2 nano-vegetable oil, and the data was collected via 5 machining parameters at 5 levels with 50 experimental runs. The ANFIS-PSO and ANFIS-GA techniques were employed to develop a model for predicting the MRR data generated during the machining operation of AL-8112 Alloy. The data were trained and tested. The expected result shows that the ANFIS-PSO training prediction rate of the MRR is 82% compared with the ANFIS GA training with 88%. When compared, the ANFIS-PSO Testing prediction rate is 80% and 81.5% for the ANFIS-GA Testing process. Therefore, the study could conclude that the MRR ANFIS-GA performed better with high accuracy. Moreover, this study will assist machinists and manufacturers in navigating their machining parameters for optimal processing and manufacturing innovation.

1. INTRODUCTION

Precision in metal machining is crucial for prototypes and final products. When a part is accurate, no mistakes could affect its mechanical operation, and it will look and feel exactly like the one created [1]. When machining, the rate at which material is removed must be measured with extreme precision. Soft computing techniques need to be implemented to model and anticipate the performances of the machining process with high accuracy and prediction analyses. MRR prediction is one of the concrete ways manufacturers can control the quality of the production of mechanical components for engineering applications [2]. Okokpujie and Tartibu [3] used a QRCC and an ANN to do a numerical analysis of the performance of a TiO_2-copra-oil-nano-lubricant with the machining parameters of MRR during the end-milling machining operation. The MRR reaction under AA8112 alloy end-milling was investigated, and about five machining parameters were considered control factors: spindle speed, feed rate, length-of-cut, cutting depth, and helix angle. A model is created for the MRR to forecast the performance of the nano-lubricants by gently raising the MRR and adjusting the machining parameters based on the measured experimental result from the end-milling machining operation. The findings indicate that raising the spindle speed decreased SR, which marginally raised the MRR during machining. A high MRR is better for an easy manufacturing process [4]. However, because of the machining parameter that caused the cutting tool and workpiece to come into contact, the end-milling operation produces heat and friction. This surplus heat results from high cutting force (CF), poor MRR, and high surface roughness (SR). Verify to identify the machining parameters and the material adhesion by using nano-lubricant having multi-walled carbon nanotube-based on copra oil to perform experimental examination with multi-objective optimisation of the machining parameters in end-milling of AL8112 alloy. The two-step method prepared the nano-lubricant, while the minimum quantity lubrication (MQL) method with five machining factors was applied to apply nano-lubricants [5].

Okokpujie and Tartibu [6] studied the MRR for improved machining of aluminium 8112 alloys. This research aims to compare the outcomes of interactions of cutting variables on copra oil-based, TiO_2- and MWCNT-based nanolubricants. The interaction between five machining parameters in three

lubrication scenarios on MRR was performed using a quadratic rotatable central composite design (QRCCD). Compared to the machining setting with MWCNTs and copra-oil-lubrication, the TiO_2 nano-lubricant improves the MRR. In conclusion, machine components for high entropy applications for sustainable production systems should be made using environmentally friendly nano-additive lubricants. In their comparative study, Azman et al. [7] showed a 12.3% decline in wear scar diameter and a 24.9% drop in coefficient of friction. The results also demonstrated that the MoS_2 nanolubricant performed the best in anti-wear and friction reduction. The graphite and hBN nanolubricants came next. The tested balls' worn surfaces were examined using microscopic and spectroscopic techniques to comprehend the lubricating mechanisms completely. Consequently, it was demonstrated that the structural alterations by sliding impacted the development of protective tribofilm. It has been proven that using nano-lubricants in machining enhances the MRR [8]. However, there is a need to implement the Heuristic and metaheuristic techniques in the prediction analysis of materials removal rate (MRR).

An expert may identify a fading inference system, or ANFIS uses output/input datasets to build a fading inference system whose membership functions are adjusted using a learning method. One of the most widely used random swarm optimisation methods is the PSO algorithm, which was inspired by the behaviour of swarm animals like fish and birds [9]. Finding the parameters that maximise or decrease the objective function under consideration is often the main task of the PSO method. An innovative hybrid approach was created during the prediction phase, integrating particle swarm optimisation (ANFIS–PSO) with an adaptive-network-based fuzzy inference system to forecast safe machining algorithms and produce practical answers for search and optimisation problems [10]. Using natural selection and genetics concepts parameters, regulate machining around several end milling operations. According to the findings, the suggested method's accuracy has considerably improved compared to alternative strategies. Additionally, using the data at hand, the efficacy of the suggested method was verified. The genetic algorithm is a computational search method for locating accurate or close solutions to search and optimisation issues [11]. GA is an approach to programming that uses biological evolution as a model to solve problems. The genetic algorithm (GA) produces practical answers for search and optimisation problems using natural selection and genetics concepts. A population of numerous individuals is developed in a GA to a state that maximises the "fitness" of the population according to predetermined selection principles. Oni-Adimabua et al. [12] employed ANFIS-based modelling to predict the accuracy of the MRR and surface roughness. The prediction results show that the ANFIS model was viable for predicting the MRR. However, the study did not consider the hybrid ANFIS-PSO and ANFIS-GA methods. Al-Ghamdi and Taylan [13] compared the prediction capabilities of the modelling approaches ANFIS and Polynomial on MRR. Two numerical parameters—current and pulse on time—and the electrode material and how it interacts with a pulse on time were deemed significant in the ANOVA concerning the polynomial model. As a result, the developed models were capable of the prediction of the MRR. However, the ANFIS model predicted the MRR more accurately.

Therefore, this study aims to develop a hybrid way of predicting the MRR during the machining of aluminium 8112 alloys by comparing the ANFIS-PSO and the ANFIS-GA. The study considered five (5) different machining parameters at five (5) levels. The parameters are the helix angle, feed rate, cutting depth, spindle speed, and cut length during the machining. MRR is one of the complex machining responses to study during the end milling process. Also, the ability to implement the ANFIS-PSO and ANFIS-GA in the prediction of MRR is a unique contribution to knowledge in machining operations.

2. MATERIALS AND METHOD

This study uses high-speed steel as the cutting tool, TiO_2 nanolubricants as cutting fluid lubricants, and Al8112 alloys as the materials. The subsections explain the methodology for data creation and the artificial intelligence tool utilised for the best prediction.

2.1 Dataset description for the MRR

The end-milling process was conducted using a five-factor, five-level experiment, and the cutting fluid was made of nano-lubricants (copra oil based on TiO_2 nanoparticles). This section is broken down into several steps. The experimental inquiry employed the subsequent methodologies. The rectangular plate made of aluminium alloy 8112 was divided into several lengths: 20, 30, 40, 50, and 60 mm. Fifty (50) samples were cut using TiO_2 nano-lubricant and copra oil lubricant, and 50 were used in each machining setting. In order to ascertain the weight before and after the machining of the workpiece, a mini-scaling system was used to weigh each of the samples. Eq. (1) calculates the MRR once the machining time is recorded and the workpiece's density is known [14].

$$MRR = (W_1 - W_2)/\rho * M_t \quad (1)$$

where, w_1 = weight before machining, w_2 = weight after machining of the AL8112 alloy (in grams), ρ = materials density of the AL8112 alloy workpiece (in g/mm^3), and M_t = machining time (minutes).

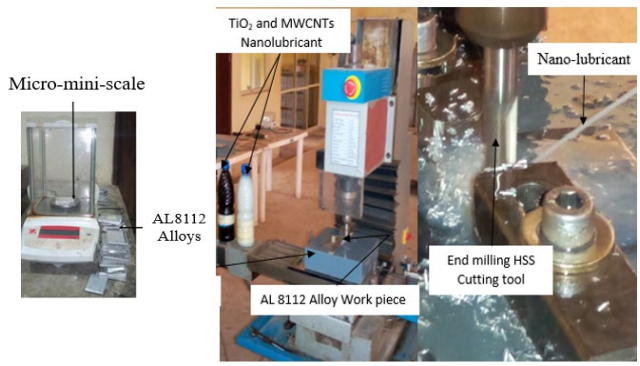

Figure 1. The machining process setup used for the data collection

This work was conducted at PEDI in Ilesha, Osun State, Nigeria, using a CNC milling system such as the SIEG 3/10/0016 desktop, which has three plane axes—the x, y, and z planes—used to experiment. Its features include a 16 mm end-milling capacity, an MT3 spindle taper, a 63 mm face-milling capacity, and a 1 kW power output. Additional

parameters include a maximum feeding speed of 500 mm/min, frequency of 50 Hz, voltage of 220-240 V, and quick movement of 2000 mm/min. Spindle travel is 270 mm, table travel is 300 × 120 mm, spindle speeds range from 100 to 5000 rpm, and the precision is 0.01 mm while repeating the process. The experimental setup utilised in this work is depicted in Figure 1.

Additionally, the necessary quantity of HSS cutting tools was used in this study to ensure that the maximum flank wear remains below the required tool wear limit of V_{Bmax} = 0.2 mm. However, the analysis only considered the cutting mode for slot milling. The TiO_2-based copra oil nano-lubricants were cleaned and placed ready for use on the vertical CNC milling machine. Additionally, the dynamometer and the Al-8112 alloy were clamped and installed on the machine's table bed, and the HSS cutting tool with a 13 mm diameter was fastened on the end milling device's spindle head.

For the machining process, CNC component programs with particular commands were created. The Y- and Z-axes employed various cut lengths, feed rates, axial depths of cuts, helix angles, and spindle speeds for each of the 50 samples. This Y- and Z-axis reference is completed. The experimental setup for end-milling the AL8112 alloy is shown in Figure 1.

2.2 Method of the prediction process for the MRR prediction via ANFIS-PSO and ANFIS-GA

Segmentation tasks, rule-based procedure controls, pattern recognition problems, and approximate function problems are included as applications of ANFIS [15]. In the ANFIS framework, which combines ANN and FL, the best way to allocate membership functions is determined through input and output data mapping connections. Adaptive network frameworks utilise some elements from fuzzy logic (FL) theory and adaptive neural networks. The FL theory enabled the development of the fuzzy interference system (FIS) application, and the FIS membership functions (MF) were progressively improved through trial and error. In the ANFIS technique, the ANN process is employed to realise the FIS model. This makes it possible for the provided data to train the neural network. Concurrently mapping the results are the factors in the Sugeno category IF-THEN rule structure. Figure 2 depicts the overall layout of the ANFIS framework. This inference system consists of five different layers. This includes the following layers: the de-fuzzy layer (iv), the fuzzy layer (i), the product layer (ii), the normalised layer (iii), and the overall output layer (v). Each stratum has unique nodes represented by squares, adaptive nodes and changeable factors. Circles, on the other hand, represent the fixed nodes, where the factors never change. Find the mathematical expression in Okokpujie and Tartibu [16].

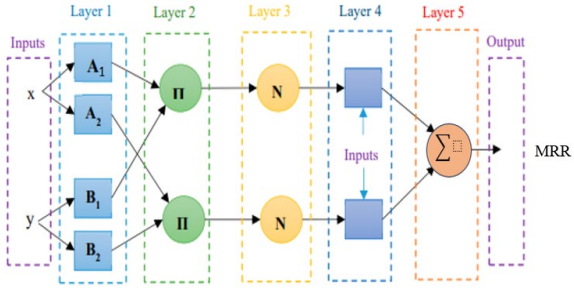

Figure 2. The architecture adopted for the ANFIS model for the MRR

The study takes into account two fuzzy if-then rules to describe the rules associated with each layer given in Eqs. (2) and (3):

$$Rule_1: if\,x\,is\,A_1\,and\,y\,is\,B_1\,then\,f = P_1x + q_1y + r_1 \quad (2)$$

$$Rule_2: if\,x\,is\,A_2\,and\,y\,is\,B_2\,then\,f = P_2x + q_2y + r_2 \quad (3)$$

A_1 and B_1 are fuzzy sets, x and y are the input variables, and f is the output (linguistic variables). As part of the ANFIS training process, the following parameters—{pi}, {qi}, and {ri}—should be measured. Each layer's performance can be evaluated using the following metrics: Initial Layer: A membership function defines each node (i) in this layer. Fuzzy logic uses membership functions to make the variables fuzzy.

The mapping from a point in the input space to a membership value in the [0,1] interval is specified by these membership functions, which are curves. There are several membership functions, the most popular being the Gaussian, Trapzoidum, and Triangular types, which give Eq. (4) and Eq. (5) [17].

$$Q_{1.i} = \sigma_{A1(x)} \quad (4)$$

$$Q_{1.i} = \sigma_{B1(x)} \quad (5)$$

where, *x* is identified as Q_1 and node input, *i* is the membership function of A_i, which the Gaussian function often defines as follows in Eq. (6):

$$\sigma_{A1(x)} = \exp\frac{-(x-c)^2}{\sigma^2} \quad (6)$$

The antecedent parameters in this formula are the standard deviation (σ) and the centre of the Gaussian membership function (C), respectively. These parameters are important for membership functions, and the optimisation algorithm determines their worth. Second Layer: The following relation determines a rule's firing strength is given in Eq. (7):

$$w_i = \sigma_{Ai(x)}\mathrm{X}\sigma_{Bi(x)} \;\; i = 1,2,\ldots \quad (7)$$

Third Layer: By dividing the projectile strength of the ith rule by the overall firing power of all rules, the firing strength of each rule is normalised in Eq. (8).

$$Q_{3.i} = \overline{w_i} = \frac{w_i}{w_1 + w_2} \;\; i = 1,2,\ldots \quad (8)$$

Fourth Layer: The fuzzy rule's outcome portion is measured in the manner described in Eq. (9):

$$Q_{4.i} = \overline{w_i}f_i = \overline{w_i}(p_ix + q_1y + r_1) \;\; i = 1,2,\ldots \quad (9)$$

where, p_i, q_i, and r_i are the consequential machining variables computed by the optimisation algorithm.

Fifty Layer: at this stage, all the outputs of the fourth layer are added to form Eq. (10), and Figure 3 depicts the MRR neural network model.

$$Q_{5.i} = \sum_{i=1}^{R} \overline{w_i}f_i \;\; i = 1,2,\ldots \quad (10)$$

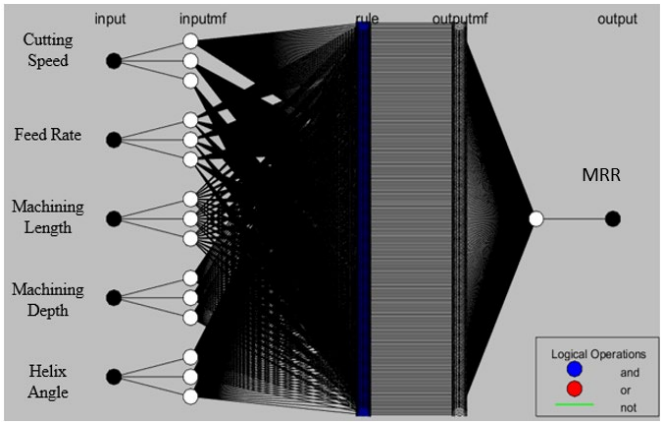

Figure 3. Neural network model for MRR

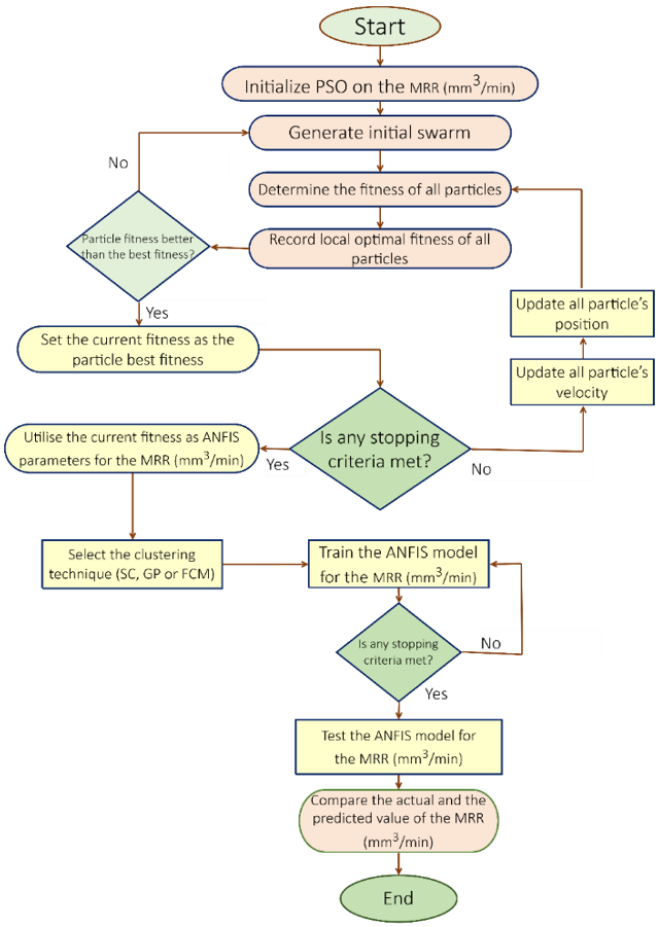

Figure 4. The procedure of the ANFIS-PSO prediction analysis

The initial and final variables are typically the two structural variables of the ANFIS model [18]. The ANFIS model's antecedent and consequent parameters are typically changed using gradient-based techniques [19]. The sluggish pace of convergence and the fact that the solution is found in local optimality are two problems with gradient-based approaches [20]. The neural network model and ANFIS structure for cutting force are displayed in Figures 3 and 4. Particle swarm optimisation (PSO) can apply metaheuristic algorithms and successfully alleviate the issues with gradient-based techniques [21]. The ANFIS-PSO method is shown in Figure 4, and the ANFIS-GA for the model utilising the metaheuristic optimisation approaches of GA and PSO is shown in Figure 5.

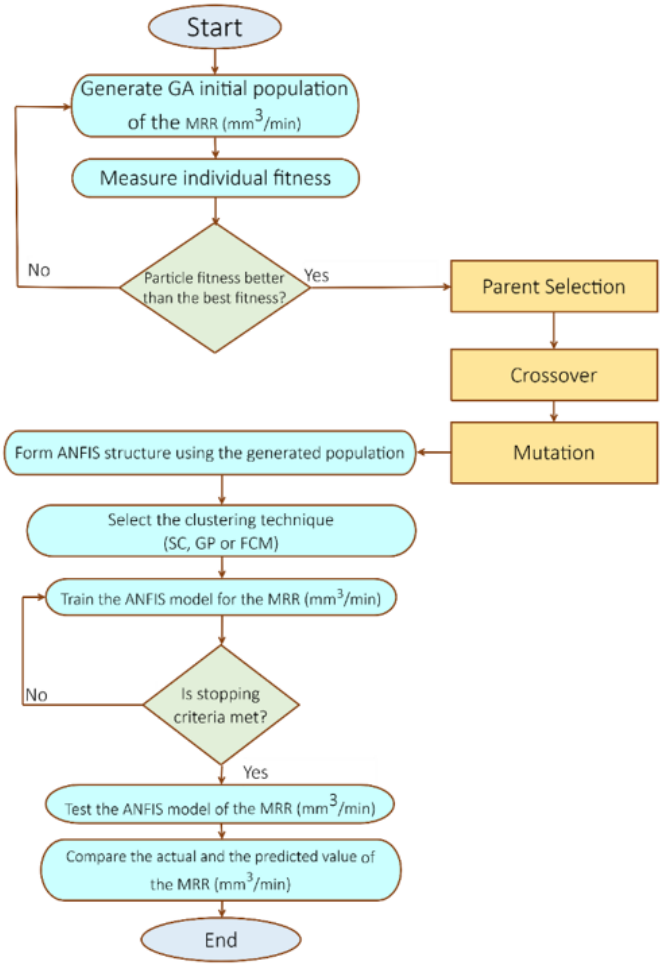

Figure 5. The procedure of the ANFIS-GA prediction analysis

In 1995, Hub and Kennedy invented the PSO algorithm, one of the nature-inspired optimisation techniques [22]. Large-scale numerical optimisation problems are primarily addressed by this method, which does not require knowledge of the target function gradient [23]. In order to solve a problem, a simple formula is used to randomly transfer a population of possible solutions into the issue domain. Subsequently, it searches for the optimal global solution (each feasible option is called a particle). Like the PSO algorithm, the approach searches inside the problem domain to produce a population of randomly produced solutions, much like the genetic algorithm [24]. The following variables were changed to perform parametric analysis after the hybrid ANN-GA model was trained using experimental data: Five to ten hidden neurones are present, depending on how the set is constructed to optimise the ANFIS using the GA algorithm, chromosome encoding, fitness function, selection, recombination, and the evolutionary scheme for the cutting force. The population numbers are 25, 50, 75, and 100.

However, the distinct GA and the PSO approach gives a random speed to each particle—that is, to every conceivable solution to the optimisation problem—so that each iteration shifts a single particle around its velocity. Moreover, unlike the genetic algorithm, every particle in the PSO algorithm should retain the superlative solution to the optimisation problem from the program's start until the end of the last iteration. The PSO algorithm can solve continuous unconstrained maximisation problems, much like the evolutionary algorithm. On the other hand, continuous state

optimisation issues (such as minimisation or maximisation) can also be solved with slight adjustments to the function specification [25]. All of these particles share five traits. The goal function that corresponds to the present location, speed, optimal position, and quantity of the objective function that corresponds to the optimal position all define the position. Within the method, equations define the position and speed of each particle. Eqs. (11) and (12), as well as based on information from the phase before. These equations designate c_1 and c_2 as the velocity constants and r_1 and r_2 as random integers. P-best, x, v, P^t, and Gt comprise inertia's weight.

$$V_{ij}^{t} = \chi\left[\omega v_{ij}^{t-1} + c_1 r_1\left(p_{ij}^{t-1} - x_{ij}^{t-1}\right) + c_2 r_2\left(G_j^{t-1} - x_{ij}^{t-1}\right)\right] \quad (11)$$

$$x_{ij}^{t} = x_{ij}^{t-1} + v_{ij}^{t} \quad (12)$$

The genetic algorithm model begins with chromosomes, a collection of solutions. A prior population is completed to generate a new one. The new solution created from the chosen progeny has a signed fitness certificate. This process is repeated Until a condition— the improvement of the best solution—is satisfied. The ANFS algorithm, which is a component of the fitness function, is crucial to f(x) in order to achieve this. Eqs. (13) and (14) show the fitness of the ANFIS algorithm function intervention.

$$f_1(x) - \frac{1}{m}\sqrt{\sum_{i}^{m} o(d_i - a_i)^2} \quad (13)$$

where, d_i is the anticipated traffic volume, a_i is the output obtained by the ANFIS, and m is the number of features.

$$f_2(x) - \frac{1}{n-m}\sqrt{\sum_{i}^{m} m(d_i - a_i)^2} \quad (14)$$

where, a_i is the actual traffic volume, d_i is the minimum, n is the total amount of input qualities, and n-m denotes the remaining undesirable characteristics.

The fitness function that follows is provided in Eq. (15).

$$f(x) - \frac{f_1(x) + f_2(x)}{2} \quad (15)$$

3. RESULTS AND DISCUSSIONS

The results obtained for the prediction analysis of the materials removal rate study on the Al8112alloys are depicted in Table 1. Fifty samples' worth of data were utilised, of which 35 runs were used for training and 15 for testing. The MRR is predicted using two hybrid metaristic models, ANFIS-PSO and ANFIS-GA. The comparative analysis of the two-hybrid system, such as the MRR ANFIS-PSO training analysis, shows that the ANFIS-PSO has a prediction rate of R^2 **0.8159**, MAPE 6.8837, MAE 3.5242, MAD 3.5164, and RMSE 4.4947.

Table 1. The performance metrics obtained for MRR via ANFIS-PSO and ANFIS GA

Performance Metrics Data	MRR ANFIS-PSO Training		MRR ANFIS GA Training	MRR ANFIS-PSO Testing	MRR ANFIS-GA Testing
Mean Absolute Percentage Error	MAPE	6.8837	5.5419	8.9155	7.6455
Mean Absolute Error	MAE	3.5242	3.3792	3.3697	3.3437
Mean Absolute Deviation	MAD	3.5164	3.4301	3.3977	3.2073
Root Mean Square Error	RMSE	4.4947	3.6685	4.0051	4.004
Coefficient of Determination	R^2	0.8159	0.8826	8031	0.8118

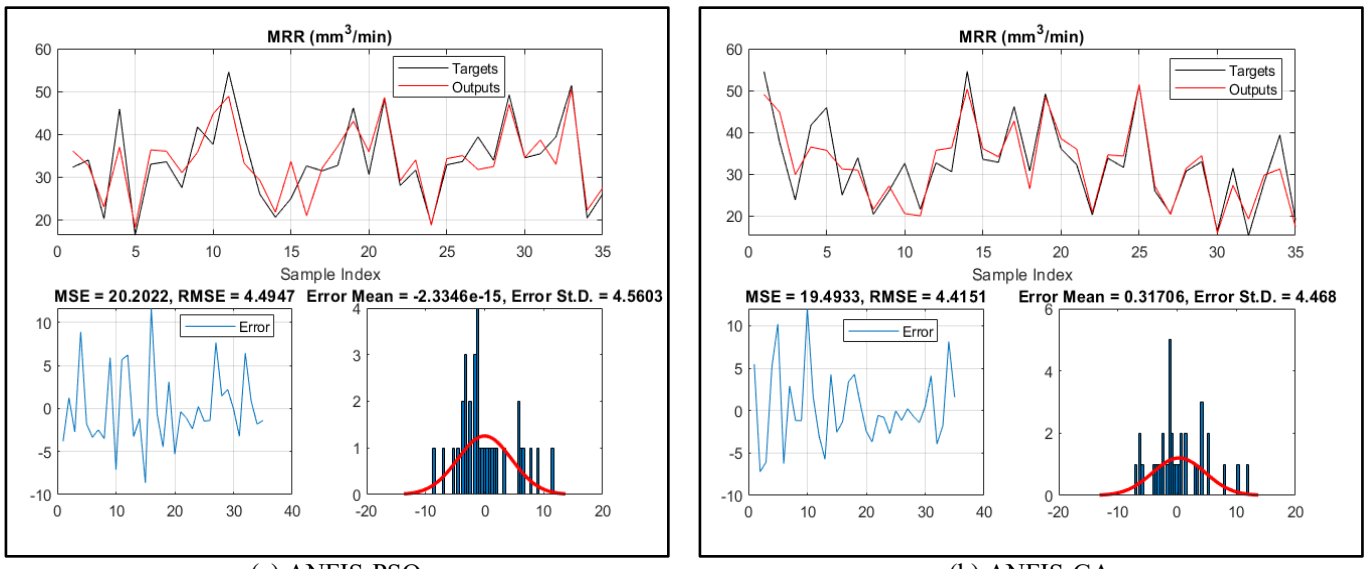

(a) ANFIS-PSO (b) ANFIS-GA

Figure 6. The comparative analysis of the training data prediction with the experimental data for the MRR

At the same time, the ANFIS-GA training performance shows that the ANFIS-GA could predict the MRR ANFIS GA training R^2 0.8826, MAPE 5.5419, MAE 3.3792, MAD 3.4301, and RMSE 3.6685. The results show that the most accurate prediction performance was achieved with the ANFIS-GA for the testing. Figure 6 shows the comparative analysis of the training data prediction with the experimental data for the MRR (a) ANFIS-PSO and (b) the ANFIS-GA. Figure 7 illustrates the comparative analysis of the training R^2 predicted and experimental data for (a) ANFIS-PSO and (b) ANFIS-GA. Figure 8 depicts the comparative analysis of the testing data prediction with the experimental data for the MRR (a) ANFIS-PSO and (b) the ANFIS-GA. Figure 9 compares the testing R^2 predicted and experimental data for (a) ANFIS-PSO and (b) ANFIS-GA.

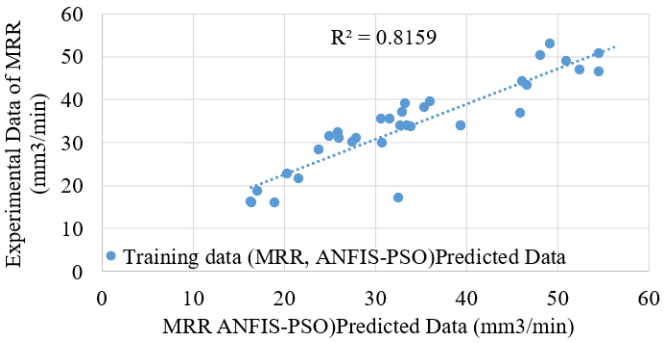

(a) ANFIS-PSO

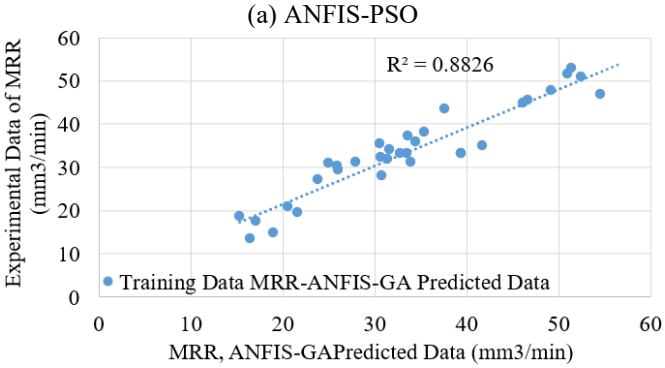

(b) ANFIS-GA

Figure 7. The comparative analysis of the training R^2 predicted and experimental data

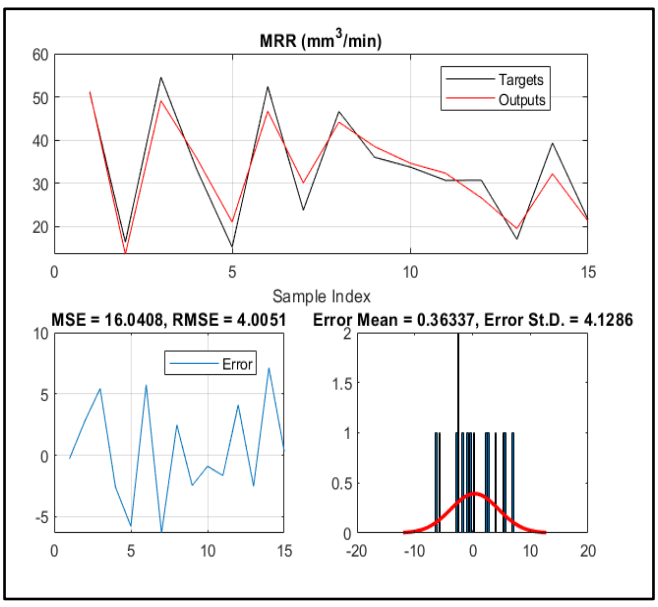

(a) ANFIS-PSO

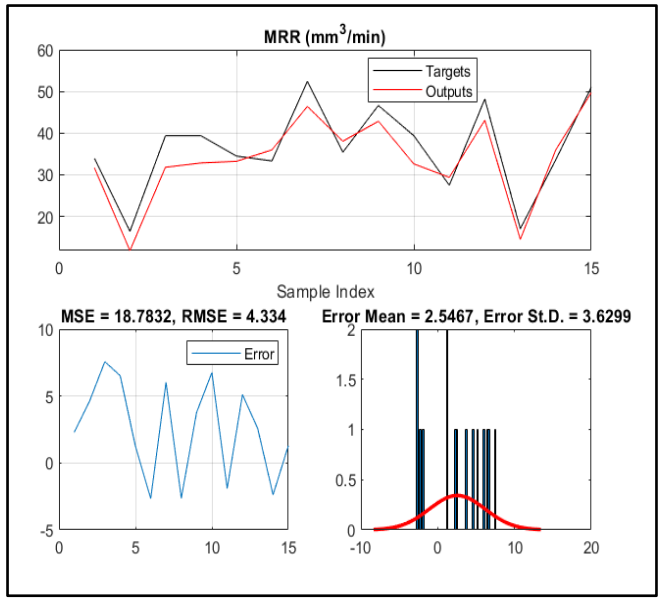

(b) ANFIS-GA

Figure 8. The comparative analysis of the testing data prediction with the experimental data for the MRR

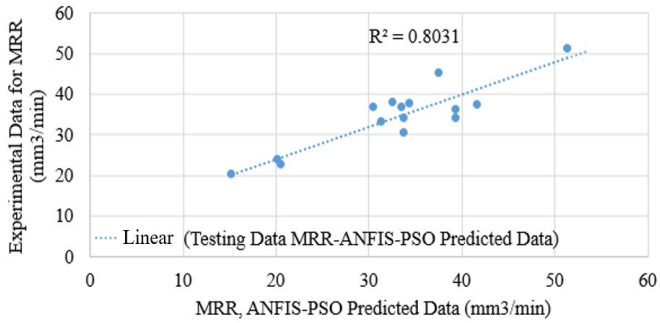

(a) ANFIS-PSO

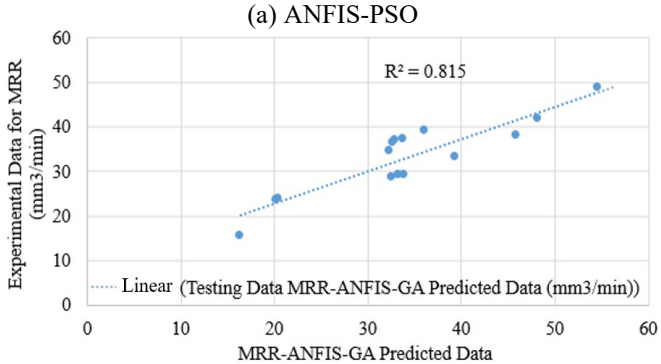

(b) ANFIS-GA

Figure 9. The comparative analysis of the testing R^2 predicted and experimental data

Statistical indicators were utilized to assess the accuracy of the model developed in this study. Eqs. (16)-(20) introduce these indicators.

$$MSE = \frac{1}{50}\sum_{i=1}^{50}(Target_i - Output_i)^2 \quad (16)$$

$$RMSE = \sqrt{\frac{1}{50}\sum_{i=1}^{50}(Target_i - Output_i)^2} \quad (17)$$

$$MAE = \sqrt{\frac{1}{50}\sum_{i=1}^{50}|Target_i - Output_i|} \quad (18)$$

$$R^2 = \left(\frac{\sum(Target_i - \overline{Target}) \times (Output_i - \overline{Output})}{\sqrt{\sum(Target_i - \overline{Target})^2 \times \sum(Output_i - \overline{Output})^2}}\right)^2 \quad (19)$$

$$STDError = \sqrt{\frac{1}{50}\sum_{i=1}^{50}(Target_i - Output_i)^2} \quad (20)$$

3.1 Comparative prediction performance of experimental results, ANFIS-PSO and ANFIS-GA of MRR of AL-8112 alloy for testing and training data

From the comparative study, Figure 10 and Figure 11 show that the ANFIS-PSO and ANFIS-GA prediction of the testing experimental data was 80%, and the ANFIS-GA was 81%, which shows that the prediction analyses are significant. MAPE of 8.9155 and 7.6455 for ANFIS-PSO Testing and ANFIS-GA Testing, respectively. Having an MAE of 3.3697 compared to 3.3437, RMSE of 4.0051 compared to 4.004 for both the MRR ANFIS-PSO Testing and the MRR ANFIS-GA Testing, this result is supported by the work [26]. The results [27] carried out a hybrid study of the ANFIS-GAN-XGBoost model for forecasting MRRs depending on process variables. This study opens the door for more research in this area by demonstrating the potential of using cutting-edge machine-learning algorithms for sustainable machining processes [28]. The ability to predict MRR for the sustainable manufacturing process is very complex as the MRR affects both the analysis of the tool wear rate, the surface produced during the machining process, and the cutting force during the cutting process. It has been proved that the application of ANFIS can predict the MRR; however, it is necessary to employ the Heuristic and Metaheuristic Methods to predict the MRR. The significant aspect of this study is to enable the application of the ANFIS-GA and ANFIS-PSO for optimal analysis of the MRR [29]. The study employed five cutting parameters with five levels to generate the data of 50 runs during the machining, and the response surface method was used to generate the experimental results for the practical study.

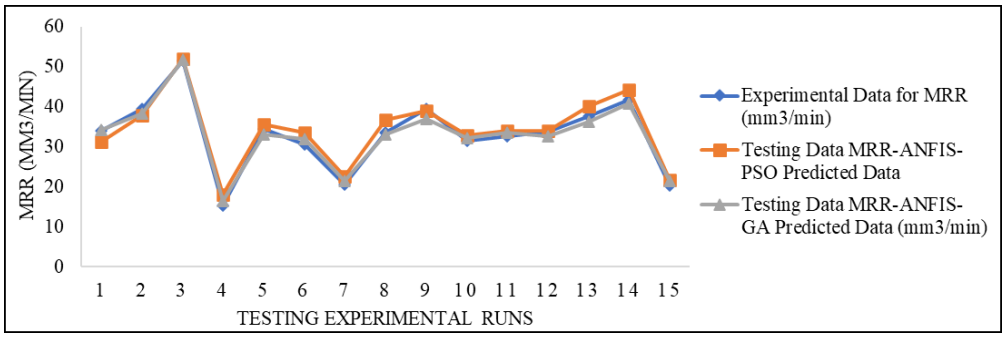

Figure 10. Comparative prediction performance of experimental results, ANFIS-PSO and ANFIS-GA of MRR of AL-8112 alloy for testing data

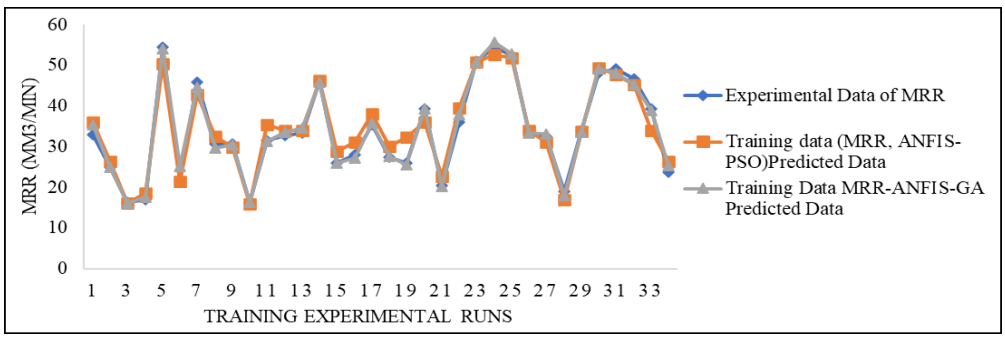

Figure 11. Comparative prediction performance of experimental results, ANFIS-PSO and ANFIS-GA of MRR of AL-8112 alloy for training data

4. CONCLUSION

The prediction analysis of the MRR of the data collected via machining of AL-8112 Alloy has been trained and tested using ANFIS-PSO and ANFIS-GA. The study considered 50 experiment runs obtained from 5 cutting parameters with 5 levels, such as helix angle, feed rate, depth of cut, spindle speed, and cut length. The spindle speed varies from 2000, 2500, 3000, 3500, and 4000 rpm, the helix angles 0, 15, 30, 45, and 60 degrees, and the feed rate 100, 150, 200, 250, and 300 (mm/min), the length of the cut, 20, 30, 40, 50, and 60 (mm), with a depth of cut 1, 1.5, 2, 2.5, and 3 (mm). Employing the response surface method to generate 50 runs for the experimental analysis. The 50 machining runs were conducted under TiO_2 nano-vegetable oil-cutting fluid machining media. The following conclusion was drawn from the results obtained from the prediction study.

-The ANFIS-PSO and ANFIS-GA techniques were viable tools for the prediction of MRR for sustainable manufacturing processes.

-The ANFIS-PSO training prediction rate of the MRR is 82% compared with the ANFIS GA training of 88%, which was achieved for the training data with the selected experimental results.

-For the testing process, the ANFIS-PSO prediction rate is 97% and 99% for the ANFIS-GA. This has shown that the hybrid model could predict the MRR for 5 cutting parameters at 5 levels.

Finally, this study will recommend that the manufacturing industry apply these parameters and techniques in machining operations for sustainable production processes. The environmental benefit of this study is that the machining operations are carried out in an eco-friendly cutting fluid environmnet, which increases the performance of the production process. For future studies, further explorations could be made into the applications in various industries, such as the study demonstrated in the construction and biomedical, respectively [29, 30].

REFERENCES

[1] Dubey, D., Singh, S.P., Behera, B.K. (2024). A review on recent advancements in additive manufacturing techniques. Proceedings of the Institution of Mechanical Engineers, Part E: Journal of Process Mechanical Engineering, 09544089241275860. https://doi.org/10.1177/09544089241275860

[2] Tian, Y., Ma, Z., Ahmad, S., Qian, C., Ma, X., Yuan, X., Fan, Z. (2024). Theoretical and experimental investigation of material removal rate in magnetorheological shear thickening polishing of Ti–6Al–4V alloy. Journal of Manufacturing Science and Engineering, 146(3): 031002. https://doi.org/10.1115/1.4063984

[3] Okokpujie, I.P., Tartibu, L.K. (2023). Material removal rate optimization under ANN and QRCCD. In Modern Optimization Techniques for Advanced Machining: Heuristic and Metaheuristic Techniques, pp. 233-262. https://doi.org/10.1007/978-3-031-35455-7_11

[4] Bui, G.T., Nguyen, Q.M., Thi, M.H.P., Vu, M.H. (2024). Multi-objective optimization for balancing surface roughness and material removal rate in milling hardened SKD11 alloy steel with SIO2 nanofluid MQL. EUREKA: Physics and Engineering, (2): 157-169. https://doi.org/10.21303/2461-4262.2024.003042

[5] Olu-lawal, K.A., Olajiga, O.K., Adeleke, A.K., Ani, E.C., Montero, D.J.P. (2024). Innovative material processing techniques in precision manufacturing: A review. International Journal of Applied Research in Social Sciences, 6(3): 279-291. https://doi.org/10.51594/ijarss.v6i3.886

[6] Okokpujie, I.P., Tartibu, L.K. (2021). Performance investigation of the effects of nano-additive-lubricants with cutting parameters on material removal rate of AL8112 alloy for advanced manufacturing application. Sustainability, 13(15): 8406. https://doi.org/10.3390/su13158406

[7] Azman, N.F., Samion, S., Paiman, Z., Hamid, M.K.A. (2024). Tribological performance and mechanism of graphite, hBN and MoS2 as nano-additives in palm kernel oil-based lubricants: A comparative study. Journal of Molecular Liquids, 410: 125616. https://doi.org/10.1016/j.molliq.2024.125616

[8] Xiao, N., Wu, C., Yang, K., Tang, J. (2024). Progress of multidimensional nano-additives under dry/liquid wear: A review. Lubricants, 12(10): 332. https://doi.org/10.3390/lubricants12100332

[9] Al-Baik, O., Alomari, S., Alssayed, O., Gochhait, S., et al. (2024). Pufferfish optimization algorithm: a new bio-inspired metaheuristic algorithm for solving optimization problems. Biomimetics, 9(2): 65. https://doi.org/10.3390/biomimetics9020065

[10] Şener, R., Koç, M.A., Ermiş, K. (2024). Hybrid ANFIS-PSO algorithm for estimation of the characteristics of porous vacuum preloaded air bearings and comparison performance of the intelligent algorithm with the ANN.Engineering Applications of Artificial Intelligence, 128, 107460. https://doi.org/10.1016/j.engappai.2023.107460

[11] Jithendra, T., Basha, S.S., Divya, A., Rajyalakshmi, G. (2024). Machine learning technique ANFIS-COA for enhancing micro-milling performance by investigating the surface roughness and material removal rate. International Journal on Interactive Design and Manufacturing. https://doi.org/10.1007/s12008-024-02061-0

[12] Oni-Adimabua, O.N., Ifeanyi-Nze, F.O., Abimbolu, A.K., Opadokun, E.O., et al. (2024). Production, optimization, and characterization of biodiesel from almond seed oil using a bifunctional catalyst derived from waste animal bones and almond shell. European Journal of Sustainable Development Research, 8(3): em0261. https://doi.org/10.29333/ejosdr/14740

[13] Al-Ghamdi, K., Taylan, O. (2015). A comparative study on modelling material removal rate by ANFIS and polynomial methods in electrical discharge machining process. Computers & Industrial Engineering, 79: 27-41. https://doi.org/10.1016/j.cie.2014.10.023

[14] Ojolo, S.J., Adjaottor, A.A., Olatunji, R.S. (2016). Experimental prediction and optimization of material removal rate during hard turning of austenitic 304l stainless steel. Journal of Science and Technology (Ghana), 36(2): 34-49. https://doi.org/10.4314/just.v36i2.4

[15] Surajudeen-Bakinde, N.T., Faruk, N., Popoola, S.I., Salman, M.A., Oloyede, A.A., Olawoyin, L.A., Calafate, C.T. (2018). Path loss predictions for multi-transmitter radio propagation in VHF bands using adaptive neuro-fuzzy inference system. Engineering Science and Technology, an International Journal, 21(4): 679-691. https://doi.org/10.1016/j.jestch.2018.05.013

[16] Okokpujie, I.P., Tartibu, L.K. (2023). Adaptive neuro-fuzzy inference system for prediction of surface roughness under biodegradable nano-lubricant. In Modern Optimization Techniques for Advanced Machining: Heuristic and Metaheuristic Techniques, pp. 289-311. https://doi.org/10.1007/978-3-031-35455-7_13

[17] Alarifi, I.M., Nguyen, H.M., Naderi Bakhtiyari, A., Asadi, A. (2019). Feasibility of ANFIS-PSO and ANFIS-GA models in predicting thermophysical properties of Al2O3-MWCNT/oil hybrid nanofluid. Materials, 12(21): 3628. https://doi.org/10.3390/ma12213628

[18] Zand, J.P., Katebi, J., Yaghmaei-Sabegh, S. (2024). A hybrid clustering-based type-2 adaptive neuro-fuzzy forecasting model for smart control systems. Expert Systems with Applications, 239: 122445. https://doi.org/10.1016/j.eswa.2023.122445

[19] Zhang, H., Sun, B., Peng, W. (2024). A novel hybrid deep fuzzy model based on gradient descent algorithm with application to time series forecasting. Expert Systems with Applications, 238: 121988. https://doi.org/10.1016/j.eswa.2023.121988
[20] Sowmya, R., Premkumar, M., Jangir, P. (2024). Newton-Raphson-based optimizer: A new population-based metaheuristic algorithm for continuous optimization problems. Engineering Applications of Artificial Intelligence, 128: 107532. https://doi.org/10.1016/j.engappai.2023.107532
[21] Chaudhari, S., Thakare, A., Anter, A.M. (2024). PSOGSA: A parallel implementation model for data clustering using new hybrid swarm intelligence and improved machine learning technique. Sustainable Computing: Informatics and Systems, 41: 100953. https://doi.org/10.1016/j.suscom.2023.100953
[22] Mottahedi, A., Sereshki, F., Ataei, M. (2018). Overbreak prediction in underground excavations using hybrid ANFIS-PSO model. Tunnelling and Underground Space Technology, 80: 1-9. https://doi.org/10.1016/j.tust.2018.05.023
[23] Qasem, S.N., Ebtehaj, I., Riahi Madavar, H. (2017). Optimizing ANFIS for sediment transport in open channels using different evolutionary algorithms. Journal of Applied Research in Water and Wastewater, 4(1): 290-298. https://doi.org/10.22126/arww.2017.773
[24] Marrel, A., Iooss, B. (2024). Probabilistic surrogate modeling by Gaussian process: A new estimation algorithm for more robust prediction. Reliability Engineering & System Safety, 247: 110120. https://doi.org/10.1016/j.ress.2024.110120
[25] Aydin, K. (2024). Comparison of regression, ANN, ANFIS, and ChatGPT prediction of turning cutting force. Journal of Engineering Design, 35(3): 338-357. https://doi.org/10.1080/09544828.2024.2311063
[26] Pang, M., Li, J., Al_Tamimi, H.M., Elkamchouchi, D.H., Ponnore, J.J., Ali, H.E. (2023). Development of hybrid ANFIS-GAN-XGBOOST models for accurate prediction of material removal rates from PCB-polluted concrete surfaces using laser technology for sustainable energy generation. Advances in Engineering Software, 184: 103500. https://doi.org/10.1016/j.advengsoft.2023.103500
[27] Adakane, R., Washimkar, P.V., Chaudhari, S.S., Giri, J., Sathish, T., Parthiban, A., Mahatme, C. (2024). Prediction and analysis of material removal rate and Tool wear for electric discharge machining of H16 material using ANN and ANOVA. Interactions, 245(1): 102. https://doi.org/10.1007/s10751-024-01933-x
[28] Okokpujie, I.P., Sinebe, J.E. (2023). An overview of the study of ANN-GA, ANN-PSO, ANFIS-GA, ANFIS-PSO and ANFIS-FCM predictions analysis on tool wear during machining process. Journal Européen des Systèmes Automatisés, 56(2): 269-280. https://doi.org/10.18280/jesa.560212
[29] Adekunle, S.A., Oyeyipo, O., Aigbavboa, C.O., Ebekozien, A., Aliu, J., Ejohwomu, O.A. (2025). A practical approach to teaching emerging technologies: A case of BIM. Engineering, Construction and Architectural Management. https://doi.org/10.1108/ECAM-10-2024-1366
[30] Ismail, R., Fitriyana, D.F., Bayuseno, A.P., Priwintoko, B., Subagyo, Y., Afrizal, M., Jamari, J., Siregar, J.P., Cionita, T., Jaafar, J. (2024). Design, fabrication, and performance testing of PMMA interference screws prepared by 3D printing methods. Journal of Advanced Research in Applied Mechanics, 128(1): 86-95. https://doi.org/10.37934/aram.128.1.8695